Received: 3 October 2019 | Revised: 9 February 2020 | Accepted: 4 March 2020

DOI: 10.1002/jrs.5875

RESEARCH ARTICLE

Journal of RAMAN SPECTROSCOPY WILEY

Noninvasive simultaneous monitoring of pH and depth using surface-enhanced deep Raman spectroscopy

Benjamin Gardner[1] | **Nicholas Stone**[1] | **Pavel Matousek**[2]

[1]School of Physics and Astronomy, University of Exeter, Exeter, UK

[2]Central Laser Facility, Research Complex at Harwell, STFC Rutherford Appleton Laboratory, Harwell Oxford, UK

Correspondence
Nicholas Stone, School of Physics and Astronomy, University of Exeter, Exeter EX4 4QL, UK.
Email: n.stone@exeter.ac.uk

Pavel Matousek, Central Laser Facility, Research Complex at Harwell, STFC Rutherford Appleton Laboratory, Harwell Oxford OX11 0QX, UK.
Email: pavel.matousek@stfc.ac.uk

Funding information
Engineering and Physical Sciences Research Council, Grant/Award Numbers: EP/K020374/1, EP/R020965/1, EP/P012442/1

Abstract

Here we demonstrate the simultaneous recovery of multiplexed physical information of surface-enhanced Raman scattering (SERS) nanoparticles (pH and depth) using deep Raman spectroscopy. As has been shown previously and in accordance with theory, inelastically scattered photons arising from spectral peaks that are suitably separated can exhibit different optical properties in the media through which they travel. These differences can impact the relative intensities of the Raman peaks as a function of the transmission path length; thereby, the depth of signal generation is inherently encoded in the spectra; assuming the target is clustered at a single depth or location, its depth can be readily determined. Moreover, Raman spectroscopy is very sensitive to chemistry of a sample, and changes in pH are observed not only as changes in peak intensity through relevant protonation and deprotonation but also as shifts in spectral features. Here, we show it is possible to precisely predict the depth (root-mean-square error [RMSE] 5 %) of SERS nanoparticles in scattering media (0.5% intralipid) while also being able to noninvasively monitor simultaneously the pH levels (RMSE ~0.2 pH units) of the media surrounding the nanoparticles. This is important as it demonstrates that nanoparticles can be used to report on multiple physical properties including their depth. This opens avenues for a range of new applications including the noninvasive diagnosis and localisation of cancer lesions in clinical environment in vivo.

KEYWORDS

deep Raman spectroscopy, depth, pH, SEDRS, SERS

1 | INTRODUCTION

The advent of deep Raman spectroscopy has led to an array of new methods for subsurface analysis of turbid media, which has impacted a number of analytical fields including pharmaceutical analysis in quality control, security applications and disease diagnosis.[1, 2] The main methods for deep probing using Raman spectroscopy originally included spatially offset Raman spectroscopy (SORS),[3] inverse SORS and transmission Raman spectroscopy (TRS)[4, 5]; however, the field is rapidly expanding with new approaches and modifications of the original concept.[6, 7]

The core concept of SORS is based on spatially separating the Raman collection and illumination zones on the surface of a diffusely scattering sample. The spectra

that are collected spatially offset from the illumination zone have differing levels of contribution between surface and subsurface chemical signals. This method allows the pure chemical signal of any specific layer and potentially its depth to be determined. However, in contrast, TRS is performed by illuminating one side of the object and collecting Raman signal from the opposing side. This approach leads to signal that constitutes all chemical species present in the sample and originally it was thought that this approach suffers from an inherent lack of depth information due to the fact that only a single measurement is performed and the Raman signals from individual depths or layers are mixed up (averaged) in the collected Raman spectrum. However, it was recently demonstrated under certain conditions, the depth of the signal could also be retrieved using TRS.[8, 9] The basis of this method of depth localisation requires the scattering matrix to have varying optical properties (e.g., μ_a) as a function of wavelength over the Raman spectral range used. Typically, this is 400–1,800 cm^{-1}, which at near-infrared wavelengths equates to ~120 nm between extremes. For biologically relevant samples, tissue and tissue phantoms, μ_a changes significantly over that range, thereby satisfying the main criterion for this approach.

Surface-enhanced Raman spectroscopy (SERS), a method for enhancing the Raman signal, can be used in combination with SORS (termed SESORS). This helps to overcome inherently weak Raman signal, which is compounded when trying to recover a Raman signal at depth in a scattering sample. To date, SESORS has mostly been used to either show conceptually a SERS signal can be recovered at depth in the range of millimetre to centimetre[10, 11] to monitor specific compounds at depth, be that glucose[12] or neurotransmitters,[13, 14] or finally to inform on other physical properties of the environment, for example, temperature or pH.[15–17] However, in these cases, the SERS reporter has been used for one function at a time, as has been a limitation in our previous studies to date.[8, 16, 18] Here we demonstrate how the spectra can be used in a multiplexed fashion to retrieve information on multiple properties simultaneously, be that the identification of SERS nanoparticles, as well as the depth and the pH using transmission Raman. This is an important step change for the field of SEDRS. In this specific case, we assume that the target molecules are confined to a single depth or location within the sample (e.g., a single cancer lesion with reporter SERS nanoparticles attached to it).

2 | MATERIALS AND METHODS

To monitor both differential transmission and pH at depth, a previously described SERS nanoparticle system was used.[15, 19] To summarise, 100-µl 1-mM mercaptobenzoic acid (MBA) was added to 1 ml of 100-nm gold nanoparticles (nanoComposix; 4.7×10^9 particles per millilitre); the solution was mixed for 8 min followed by centrifugation at 5,000 rpm for 10 min. The supernatant was then removed, and the gold-labelled nanoparticles (Au-MBA) were resuspend in 1× phosphate buffered saline solution. A quartz cell (Cell 1) with a 2-mm internal path length (internal volume 0.7 ml) contained the Au-MBA nanoparticles; this was centrally aligned to the x axis and moved along the z axis in ~2-mm steps by a motorised translation stage (Standa Ltd) through a larger quartz cell (45 × 45 × 30-mm external dimensions) with the total internal optical path length (~26 mm; Cell 2). Cell 2 contained a predominantly diffusely scattering intralipid solution (Sigma-Aldrich) at 0.5% (reduced scattering coefficient of ~μ_s' 4.6 cm^{-1}). Raman spectra were recorded for a series of z steps at multiple pH levels; for each pH level (six in total), Cell 1 was translated through nine positions within Cell 2 (Figure 1).

Experiments were carried out on a previously described home-built deep Raman system operating in transmission mode.[20] The laser excitation wavelength was 830 nm (Innovative Photonic Solutions:

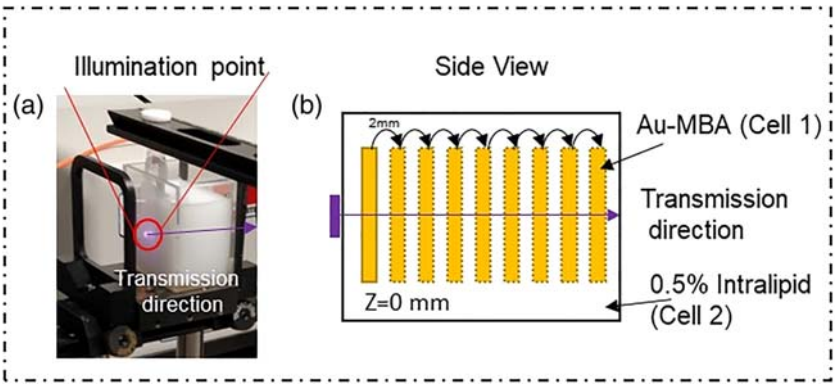

FIGURE 1 (a) A photo of the transmission Raman experimental set-up, with the illumination point on the sample highlighted and the trajectory of the sample signal highlighted. (b) Schematic of the experimental design as observed from the side demonstrating fixed-point transmission illumination and the movement of Cell 1 containing nanoparticles through the larger Cell 2 filled with intralipid solution [Colour figure can be viewed at wileyonlinelibrary.com]

I0830MM0350MF-EM) delivering ~350 mW at the sample surface with a beam diameter of ~2 mm. Raman spectra were collected from the other side of the sample from an area of approximately 2-mm diameter and relayed via an optical system to a Kaiser spectrometer (Holospec 1.8i) with a deep depletion charge-coupled device camera (Andor iDus-420). Raman spectra were measured for 5 s × 60 accumulations, at each depth, in all experiments.

The Raman spectra were processed using MATLAB 2014a. The spectra underwent minimal processing limited to calculating averages at each spatial point. A principal component analysis (PCA) model of pH changes was constructed from the average spectra; the data were truncated to the spectral region of interest and scaled to [0–1]. Data, acquired at depth, underwent the same process. For determining peak ratios, the spectra were additionally processed by applying a baseline correction using asymmetric least squares approach.[21, 22]

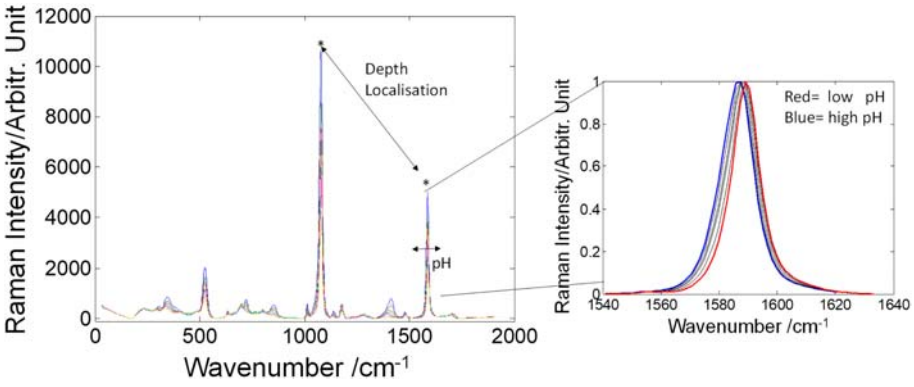

FIGURE 2 Pure Raman spectra of Au-mercaptobenzoic acid nanoparticles measured at six pH levels with ~0.5 pH intervals between each measurement. The two most intense Raman bands are highlighted, where the relative intensity of the peaks can be used to predict depth, and the position of the higher wave number Raman band for pH sensing [Colour figure can be viewed at wileyonlinelibrary.com]

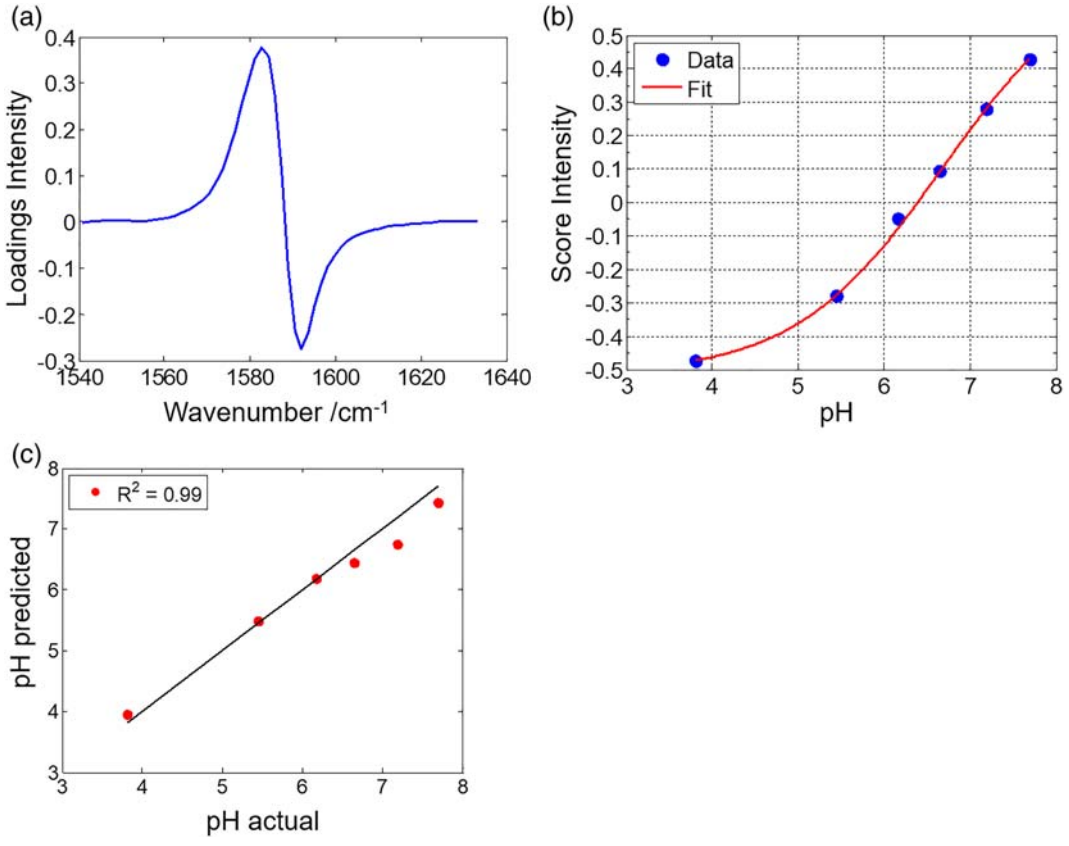

FIGURE 3 (a) The loading intensity of PC1 of Au-mercaptobenzoic acid nanoparticles Raman spectra measured at six pH levels for the relevant spectral window of 1,540–1,630 cm^{-1}. (b) PC1 score intensities as a function of pH, fitted with a sigmoidal Boltzmann function. (c) pH actual of the Au-mercaptobenzoic acid nanoparticles versus the predicted pH when measured at depth in 0.5% intralipid [Colour figure can be viewed at wileyonlinelibrary.com]

3 | RESULTS AND DISCUSSIONS

The Raman spectra of the Au-MBA nanoparticles are shown (Figure 2), displaying the full spectral range, with the peaks used for simultaneous pH monitoring and depth localisation highlighted. As has been demonstrated previously,[8] photons of different wavelengths that travel through a matrix (e.g., intralipid, tissue and water), with changing optical properties (μ_a and μ_s) as a function of wavelength, experience differing levels of absorption and scattering as they migrate through the material. Spectrally in deep Raman of biological tissues, where typical photon path lengths are relatively high (millimetre to centimetre), this phenomenon is observed as relative intensity differences between suitably separated Raman peaks as a function of distance from Raman photon creation and Raman collection zone. Therefore, the spectra inherently encode for the localised position of the Raman creation event, when the conditions of differential transmittance of the matrix and spectral separation are satisfied. In this example, the spectral separation of ~43 nm between the highlighted Raman bands (Figure 2) is sufficient to distinguish depths over a 26-mm transmission distance, through changes in the relative intensity of Raman bands 1,085 and 1,587, (ν_{12} ring stretching and ν_8 ring breathing, respectively). Moreover, as is also shown (Figure 2), the ν_8 ring breathing mode is sensitive to changes in pH, with a shift to lower wave numbers with increasing pH, which can be used independently to inform on pH[23] from the same depth.

A PCA model of the peak positional change of Au-MBA nanoparticles over a series of pH levels measured in a bare vial (i.e., not at depth) was first constructed. Figure 3a shows the loadings of PC1 for the spectral range 1,540–1,630 cm^{-1}, which is characteristic of peak positional change. The score intensities for PC1 were fitted using a sigmoidal Boltzmann fit (Figure 3b), with $R^2 = .99$. The spectra measured at depth (in Cell 2 filled with intralipid solution) were then projected onto the PCA model, and the pH was predicted. Figure 3c shows that there is a strong relationship between the predicted pH calculated from PC scores, as shown on the *y* axis and actual pH measurements shown on the *x* axis. This translates as an RMSE of 0.23 pH units, which demonstrates that pH can be predicted with suitable accuracy for clinical benefit.

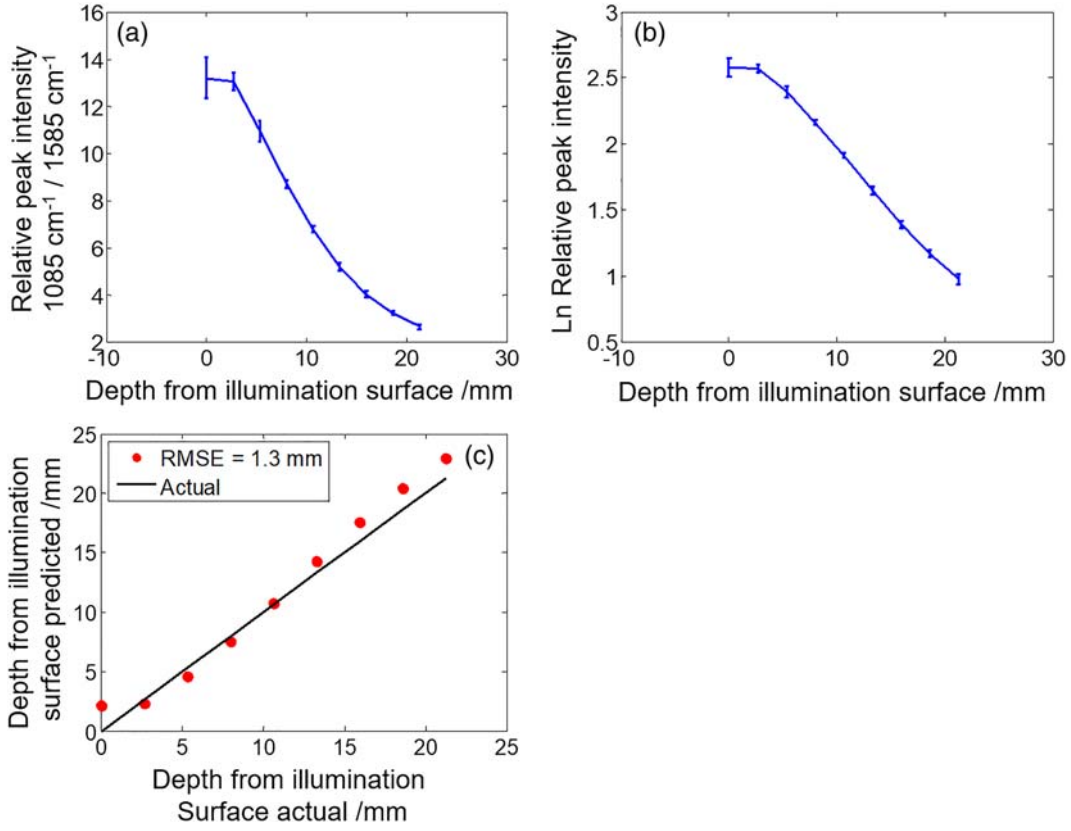

FIGURE 4 (a) The relative intensity of selected Au-mercaptobenzoic acid Raman bands (1,085 and ~1,585 cm^{-1}) with increasing depth from the illumination surface. (b) The natural logarithm of the relative peak intensity with increasing depth from illumination surface. (c) The predicted depth of the Au-MBA nanoparticles from two external calibration points [Colour figure can be viewed at wileyonlinelibrary.com]

As discussed above, relative intensity changes encode the depth (Figure 4a), as Cell 1 travels through cell 2, and the path length decreases between Raman creation and collection zone, and it is observed that the relative intensity between the two Raman peaks (1,085 and 1,585 cm^{-1}) decreases. When the natural logarithm of the relative intensity change is displayed with creation depth (Figure 4b), it can be seen that there is a mostly linear relationship between the depth of illumination and the peak relative intensity change. Therefore, through measuring the pure signal of the Au-MBA nanoparticles, and the signal of the nanoparticles passing through the entirety of the matrix, that is, Cell 2 filled with intralipid, it is possible to predict the depth on the basis of just two external calibration points (Figure 4c). As is shown along the x axis is the actual depth of the cell containing the Au-MBA nanoparticles, whereas the y axis shows the predicted depth based upon external calibration. It was possible using the discussed calibration approach to predict the depth of the Au-nanoparticles with an error (RMSE) of 1.3 mm.

4 | CONCLUSIONS

Here we have demonstrated how by using SEDRS that it is possible to simultaneously monitor pH and location of these at depth in a scattering sample using only external calibration procedures and no a priori information. This is a critical development for not only the rapidly expanding deep Raman field, demonstrating how information rich the approach is, but also demonstrating how nanoparticles can be used with their final practical application in mind, to not only be monitored, but monitor physical properties at depth and determining their location.

ACKNOWLEDGEMENT

EPSRC grants (EP/K020374/1, EP/P012442/1 and EP/R020965/1) partly funded the work presented here.

ORCID

Benjamin Gardner https://orcid.org/0000-0002-7223-9585
Nicholas Stone https://orcid.org/0000-0001-5603-3731
Pavel Matousek https://orcid.org/0000-0003-0912-5339

REFERENCES

[1] P. Matousek, N. Stone, *Chem. Soc. Rev.* **2016**, *45*, 1794.
[2] J. R. Maher, J. A. Inzana, H. A. Awad, A. J. Berger, *J. Biomed. Opt.* **2013**, *18*, 077001.
[3] P. Matousek, I. P. Clark, E. R. C. Draper, M. D. Morris, A. E. Goodship, N. Everall, M. Towrie, W. F. Finney, A. W. Parker, *Appl. Spectrosc.* **2005**, *59*, 393.
[4] B. Schrader, G. Bergmann, *Fresenius' Zeitschrift für Anal. Chemie* **1967**, *225*, 230.
[5] P. Matousek, M. D. Morris, *Emerging Raman Applications and Techniques in Biomedical and Pharmaceutical Fields*, Springer, Berlin Heidelberg, Berlin, Heidelberg **2010**.
[6] S. K. V. Sekar, S. Mosca, A. Farina, F. Martelli, P. Taroni, G. Valentini, R. Cubeddu, A. Pifferi, *Opt. Express* **2017**, *25*, 4585.
[7] K. M. Khan, S. K. Majumder, P. K. Gupta, *J. Biophotonics* **2015**, *8*, 889.
[8] B. Gardner, N. Stone, P. Matousek, *Anal. Chem.* **2017**, *89*, 9730.
[9] S. Mosca, P. Dey, T. A. Tabish, F. Palombo, N. Stone, P. Matousek, *Anal. Chem.* **2019**, *91*, 8994.
[10] S. M. Asiala, N. C. Shand, K. Faulds, D. Graham, *ACS Appl. Mater. Interfaces* **2017**, *9*, 25488.
[11] N. Stone, M. Kerssens, G. R. Lloyd, K. Faulds, D. Graham, P. Matousek, *Chem. Sci.* **2011**, *2*, 776.
[12] K. Ma, J. M. Yuen, N. C. Shah, J. T. Walsh, M. R. Glucksberg, R. P. Van Duyne, *Anal. Chem.* **2011**, *83*, 9146.
[13] A. S. Moody, P. C. Baghernejad, K. R. Webb, B. Sharma, *Anal. Chem.* **2017**, *89*, 5688.
[14] B. Sharma, A. S. Moody, in *Advanced Photonics 2017 (IPR, NOMA, Sensors, Networks, SPPCom, PS)*, Optical Society of America, **2017**, p. SeTu2E.5.
[15] B. Gardner, N. Stone, P. Matousek, *Faraday Discuss.* **2016**, *187*, 329.
[16] B. Gardner, P. Matousek, N. Stone, *Anal. Chem.* **2019**, *91*, 10984.
[17] B. Gardner, P. Matousek, N. Stone, *Analyst* **2019**, *144*, 3552.
[18] M. Z. Vardaki, H. Sheridan, N. Stone, P. Matousek, *Appl. Spectrosc.* **2017**, *71*, 1849.
[19] L. E. Jamieson, A. Jaworska, J. Jiang, M. Baranska, D. J. Harrison, C. J. Campbell, *Analyst* **2015**, *140*, 2330.
[20] M. Z. Vardaki, B. Gardner, N. Stone, P. Matousek, *Analyst* **2015**, *140*, 5112.
[21] P. H. C. Eilers, *Anal. Chem.* **2003**, *75*, 3631.
[22] P. H. C. Eilers, H. F. M. Boelens, *Leiden University Med. Center Rep.* **2005**, 1.
[23] A. Williams, K. J. Flynn, Z. Xia, P. R. Dunstan, *J. Raman Spectrosc.* **2016**, *47*, 819.

How to cite this article: Gardner B, Stone N, Matousek P. Noninvasive simultaneous monitoring of pH and depth using surface-enhanced deep Raman spectroscopy. *J Raman Spectrosc*. 2020;51: 1078–1082. https://doi.org/10.1002/jrs.5875